Propellants, Explosives, Pyrotechnics 11, 144–149 (1986)

Measurement of Shock Initiation Threshold of HNAB by Flyer Plate Impact

E. Hasman, M. Gvishi, and Y. Carmel

Government of Israel, Department of Science, Haifa (Israel)

Messung der Stoßzündschwelle von HNAB durch Aufschlag einer Flugplatte

Es wurde die Stoßzündschwelle vom Explosivstoff Hexanitroazobenzol (HNAB) ermittelt unter Verwendung von durch den Aufschlag einer Flugplatte erzeugten Druckimpulsen. Die Platte wurde von einer elektrisch explodierbaren Metallfolie (elektrische Kanone) bis zu einer Geschwindigkeit von 2.5 mm/µs beschleunigt. Der dadurch erzeugte Stoßdruck P betrug bis zu 7.3 GPa; die Druckdauer (Stoßdauer) τ variierte zwischen 40 ns und 210 ns.

Es wurde ein halb-empirisches Modell zur Beschreibung des Verfahrens der explodierenden Folie entwickelt. Die Übereinstimmung des Modells mit den Versuchsergebnissen war zufriedenstellend. Es hat sich herausgestellt, daß je länger die Druckdauer war, desto stärker war die Abweichung der Zündschwellenkurve von $P^2\tau$ = const. Bei langen (200 ns) Impulsen wird der konstante Druck zum Zündkriterium; sein Wert war 2.9 GPa bei 1.6 g/cm³, bei einer Korngröße von 5 µm. Der Einfluß der Explosivstoff-Dichte und der Korngröße auf die Zündschwelle läßt sich durch „hot spots" und die Porosität des Explosivstoffes erklären. Aus den Versuchsergebnissen konnte die kritische Energie der Zündschwelle abgeleitet werden. Sie betrug 12 J/cm² für eine 76 µm-dicke Flugplatte und eine Korngröße von 5 µm.

Mesure du seuil d'amorçage par choc de l'hexanitrozazobenzène (HNAB) par impact d'une plaque

On a cherché à déterminer le seuil d'amorçage de l'explosif hexanitroazobenzène (HNAB) sous l'effet du choc engendré par l'impact d'une plaque. La plaque a été lancée à une vitesse de 2,5 mm/µs sous l'effet de l'explosion d'une feuille métallique (canon électrique). La pression P du choc atteint jusqu'à 7,3 GPa et sa durée τ varie entre 40 ns et 210 ns.

On a mis au point un modèle semi-empirique pour décrire le processus d'explosion d'une feuille métallique. Le résultat fourni par ce modèle concorde de manière satisfaisante avec les données expérimentales. Il est apparu que plus la durée d'application de la pression est grande, plus la courbe du seuil d'amorçage s'écarte de $P^2\tau$ = const. Avec des impulsions de longue durée (200 ns), le palier de pression constitue le critère d'amorçage; ce palier se situe à 2,9 GPa pour 1,6 g/cm³ et une granulométrie de 5 µm. L'influence de la masse volumique de l'explosif et de sa granulométrie s'explique par l'apparition de points chauds et par la porosité de la substance. A partir des résultats expérimentaux on a pu déterminer l'énergie critique nécessaire à l'amorçage. Elle était de 12 J/cm² pour l'impact d'une plaque de 76 µm d'épaisseur et une granulométrie de l'explosif de 5 µm.

Summary

The shock initiation threshold of HNAB (Hexanitroazobenzene) explosive has been measured using pressure pulses generated by flyer plate impact. The flyer plates were accelerated by an electrically exploded metallic foil (electric gun) up to velocity of 2.5 mm/µs generating impact pressures, P, up to 7.3 GPa lasting between τ = 40 ns to 210 ns, where τ is the duration of the impact.

One dimensional semi-empirical model was developed to describe the exploding foil process. We found a good agreement between the semi-empirical model and the experimental data. It was found that as the pressure duration gets longer, the initiation threshold curve swings away from the $P^2\tau$ = constant. For long (200 ns) pulses, the initiation criterion becomes one of a constant pressure. This constant threshold pressure is 2.9 GPa at 1.6 g/cm³ (grain size is 5 µm). The effect of the explosive density and grain size on initiation threshold can be explained by hot spots and porous explosive concept. A critical energy for initiation threshold of 12 J/cm² was derived from our measurements (with flyer thickness 76 µm and grain size 5 µm).

1. Introduction

Explosive materials are utilized in a number of systems in the area of terminal ballistics. Effective design and performance analysis of a system employing explosive materials are dependent upon good knowledge of initiation threshold of the explosive, as well as other factors like thermodynamic behavior, stability, etc.

The purpose of this work was to study the shock initiation threshold[1] of HNAB to impact pressure. HNAB is of interest due to its high melting point (~220 °C) and relative insensitivity as compared to PETN and HNS (Drop Hammer Test[2]). However, little is known about its initiation characteristics by planar shock waves[3]. In this work, we have concentrated on shock initiation by very short duration pulses with pulse length varying from 40 ns to 200 ns. We were particularly interested in the initiation threshold dependence on grain size, flyer diameter, shock duration, pressure and explosive density[4].

The electric gun is a versatile tool for such high pressure short shock wave research. Only small quantities (<1 g) of explosive are required for testing, so the testing can be done in an enclosed firing tank with good diagnostic access and quick experimental turn around.

The electric gun[5] produces as well characterized shock stimulus. Flyer plates were accelerated by an electrically exploded metallic foil up to a velocity of 2.5 mm/µs, generating pressures up to 7.3 GPa upon impact with the HNAB samples.

The research objectives were:

(1) Development of an electric gun for high impact studies.
(2) Comparison between the gun experimental parameters (such as electrical parameters and flyer's velocity) and a one-dimensional semi-empirical model.
(3) Studies of shock initiation threshold of HNAB under various impact pressures produced by the electric gun.

2. The Electric Gun and Diagnostics Technique

Experiments were conducted to study the effect of density, morphology, grain size, flyer diameter and pulse duration on

0721-3115/86/0510-0144$02.50/0

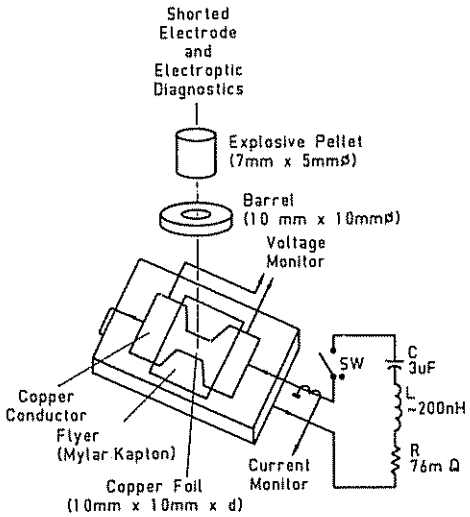

Figure 1. Schematic diagram of electric gun.

the shock initiation threshold of HNAB, using an electric gun similar to the one previously described by Chau et al.[5].

The electric gun (slapper) was usually composed of copper foil (thickness 8 μm, area 1 mm × 1 mm), and polyimide or polyester flyer (Fig. 1). The flyer diameter was defined by a 1 mm diameter brass barrel (1 mm long) which was clamped onto the foil flyer laminate. The electrical firing system consisted of a 3 μF capacitor charged up to 5.5 kV DC.

The inductance L and the resistance R of the equivalent circuit (see Fig. 1) including the foil, dictates an underdamped oscillatory current waveform. Flyers velocities up to 2.5 mm/μs were measured by electric (shorted-electrode method) and electroptic methods, allowing calibrating of the Gurney model[6].

Figure 2 shows the burst current I_b through the cross section of the foil as a function of the capacitance charging voltage. This data enables us to calculate the final flyer velocity V_f, (Fig. 3) as a function of J_b, the burst current density into the foil by the following equation:

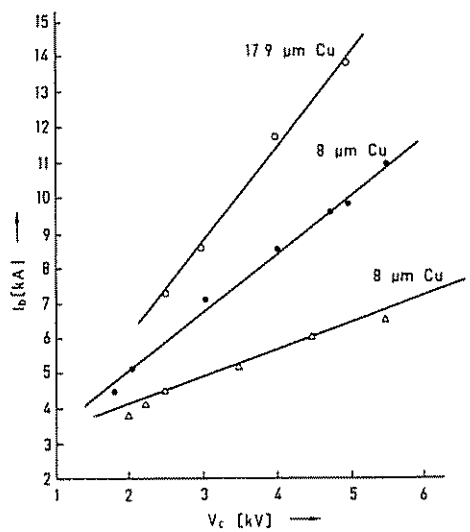

Figure 2. The variation of burst current of the foil with capacitance charging voltage. ○ – thickness – 17.9 μm and 1 mm × 1 mm. • – thickness – 8.0 μm and 1 mm × 1 mm. △ – thickness – 8.0 μm and 0.5 mm × 0.5 mm.

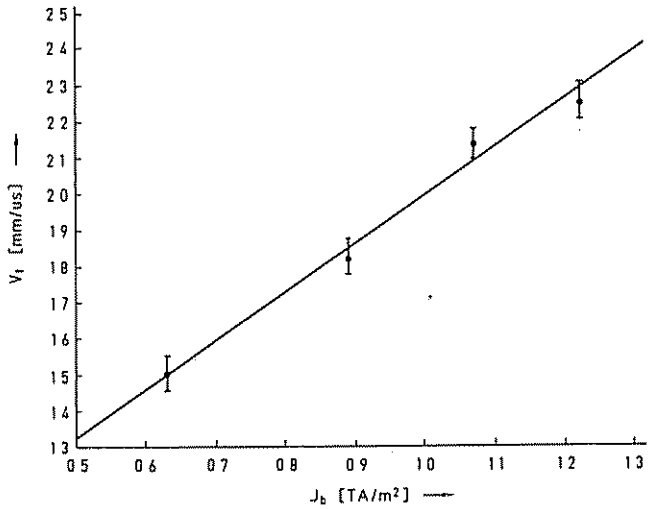

Figure 3. Flyer velocity, V_f, versus burst current density J_b. Copper foil thickness – 8 μm. Mylar flyer thickness – 76 μm.

$$V_f = (1.765\ J_b + 0.918)\left(\frac{M}{C} + \frac{1}{3}\right)^{-\frac{1}{2}} \quad (1)$$

In Eq. (1), J_b is expressed in TA/m^2, C is the mass of the copper foil per unit area and M, is the flyer mass per unit area.

3. Semi-empirical Model for Exploding Foil

A one-dimensional semi-empirical model was used to describe the mechanism of foil explosion, using the following assumptions[7]:

(1) The volume of the exploding foil is constant up to the burst time.

(2) The foil's specific resistivity, changes linearly with temperature up to the exploding temperature T_b, while the ratio R_b/R_o is characteristic constant for each foil material, and was experimentally found to be $R_b/R_o \simeq 120$ for copper. Using that, we can show that the current density J (t) and the burst time t_b satisfy the action integral:

$$g = \int_0^{t_b} J^2(t)\,dt \simeq \text{const.} \quad (2)$$

(3) The equation of state was based on a semi-empirical model for the internal energy $\varepsilon = \varepsilon(T, V)$. V is the specific volume and T is the temperature.

The internal energy equation, ε, contains three components: The elastic energy, ε_c (low temperature component), which was neglected in the numerical calculation, the thermal energy of atoms ε_{ia} and the electronic contribution ε_{el} especially important at high temperature.

(4) The duration of the explosion process is much shorter than the time of energy's dissipation in the foil. Heat conductance, radiation losses, and heat of phase transformation are all neglected.

We assumed that all the electric energy delivered to the foil was converted to Joule heating in the Cu-foil. Moreover, the current distribution through the cross section of the foil assumed to be uniform, (the skin depth was over 70 μm and sample thicknesses were between 8 μm to 18 μm). The one-dimensional semi-empirical model which was used to describe the exploding foil mechanism neglected temperature gradients within the foil.

The equations of semi-empirical model are as follows:

$$\partial Q/\partial t = J^2/\sigma_f(t)\ \varrho\ (t) \tag{3}$$

$$r_f(t) = r_{fo}[I + \alpha(T(t) - To)] \tag{4}$$

$$LdI/dt + RI + r_f(t)\ I + (1/C)\left(\int_0^t I(\lambda)\, d\lambda + q_o\right) = 0 \tag{5}$$

$$Q = \varepsilon(T, V) - \varepsilon(T_o, V_o) \tag{6}$$

Q – Heat capacity per unit mass of the metal foil.
J – Current density through the foil's cross section.
σ – Electric conductivity.
ϱ – Mass density.
r_{fo}, r_f – The initial and dynamic resistivities of the foil.
T_o, T – Ambient and dynamic (time varying) temperatures respectively.
α – Linear resistance coefficient.

Equation (3) describes the ohmic heating in the foil, while its time dependent resistance is given by Eq. (4), assuming a linear resistance coefficient. The current in the circuit is described by Eq. (5), where q_o is the initial charge on the capacitor C. Equation (6) is the equation of state of the foil material as a function of temperature and the specific volume V.

The energy equation (6) can be written as followed[8]:

$$\varepsilon(V, T) = \varepsilon_c(V) + \varepsilon_{la}(V, T) + \varepsilon_{el}(V, T) \tag{7}$$

The calculation of the thermal energy of ions usually described by

$$\varepsilon_{la} = C_v(T) \cdot T \tag{8}$$

Where $C_v(T)$ is the specific heat capacity and from the first assumption is only a function of T. This equation is very simple at low temperature, where we have six degrees of freedom.

$$\varepsilon_{la} \simeq 6 \times 1/2\ NKT = 3\ NKT \tag{9}$$

where K is Boltzmann's constant, and N is the number of atoms per unit mass.

At high temperature we have three degrees of freedom and

$$\varepsilon_{la} = 3 \times 1/2\ NKT = \frac{3}{2} NKT \tag{10}$$

At the intermediate temperatures (semi-liquid phase) Altshuler[9] derived the following Eq. (11) by interpolation to low and high temperatures.

$$\varepsilon_{la}(V, T) = \frac{\left(2 + \frac{\ell}{C^2} RT\right)}{\left(1 + \frac{\ell}{C^2} RT\right)} \times \frac{3}{2} KN(T - T_o) + \varepsilon_o \tag{11}$$

where R is the gas constant, C is the speed of sound C (T = o) = 3921 m/s, ℓ is an empirical parameter, $\ell = 9$ for copper in C.G.S, ε_o is the internal energy at room temperature.

It is known[8,9] that the electronic contribution for $T < 50000$ K is

$$\varepsilon_{el} = 1/2\ \beta_o \left(\frac{V}{V_o}\right)^{\frac{1}{3}} T^2 \tag{12}$$

where β_o is 110 erg/g · k^2.

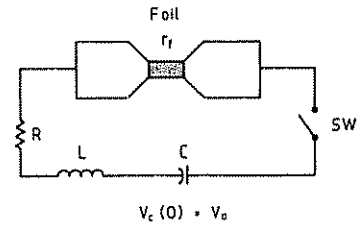

Figure 4. The equivalent circuit of the electric gun.

From Eq. (11, 12) we can calculate the contribution of thermal energy (ionic part) and electronic contribution (electron part) to the total pressure using Grüneisen approximation[8].

Equations (3–6) were solved using computer code[7]. The parameters of a typical experiment are: Cu-foil with 8 μm thickness,

$$(di/dt)_{t=0} = V_c/L = 4\ kV/200\ nH\ ,$$

$$r_{fo} = 2.15\ m\Omega\ , \qquad R_b = 2.15 \times 120 = 259\ m\Omega$$

$$C = 3\ \mu F \qquad \text{and} \qquad \alpha = 0.003\ (K^{-1})\ .$$

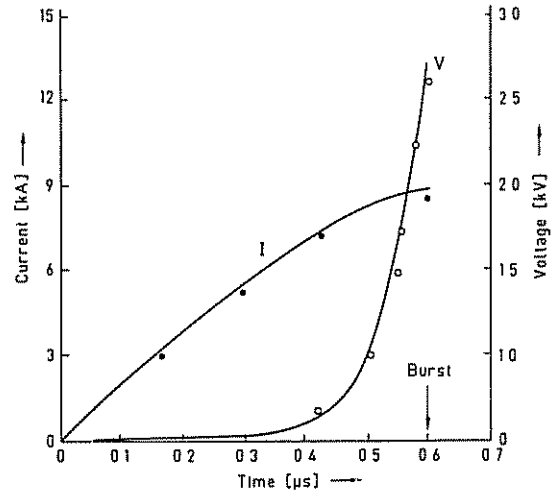

Figure 5. The calculated current I (t) and V (t), (solid lines) are compared to measured value (dots) for one representative experiment.

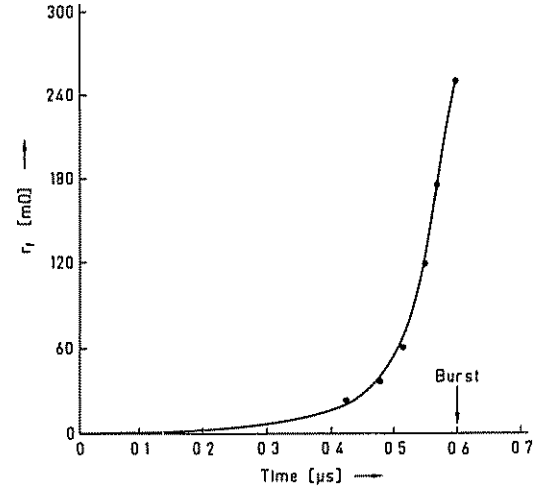

Figure 6. The calculated dynamic resistance of the foil $r_f(t)$, (solid line) compared to measured values (dots) for one representative experiment

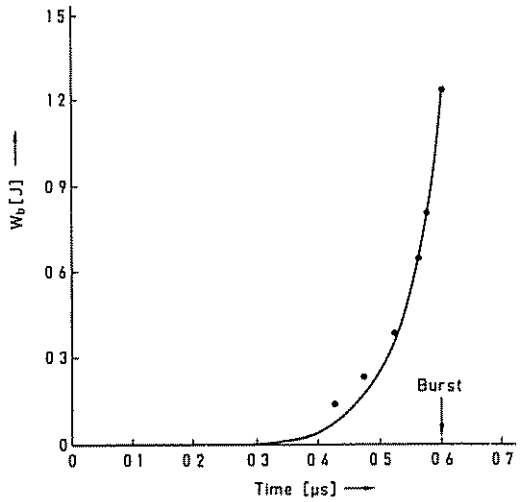

Figure 7. The calculated electrical energy $W_b(J)$, (solid line) compared to measured values (dots) for one representative experiment.

Figures 5, 6 and 7 compare the measured and calculated current, I(t), voltage V(t), dynamic resistance, $r_f(t)$, and electrical energy $W_b(t)$, values for our representative experiment.

4. Results and Discussion

We used in our experiments pellets of HNAB explosive which were synthesized in a step process as previously described by Hasman et al.[4].

Many experiments were performed in order to ensure good statistics for the initiation threshold data. In each experiment we measured the foil's current and voltage waveforms.

The effect of explosive density between 1.15 g/cm^3 to 1.67 g/cm^3 on threshold burst current and power are shown in Figs. 8 and 9. The experimental points represent the statistical initiation threshold of the explosive (50% detonation of the explosive). No difference was found[4] between the threshold sensitivity of the two polymorphic phases HNAB (I, II).

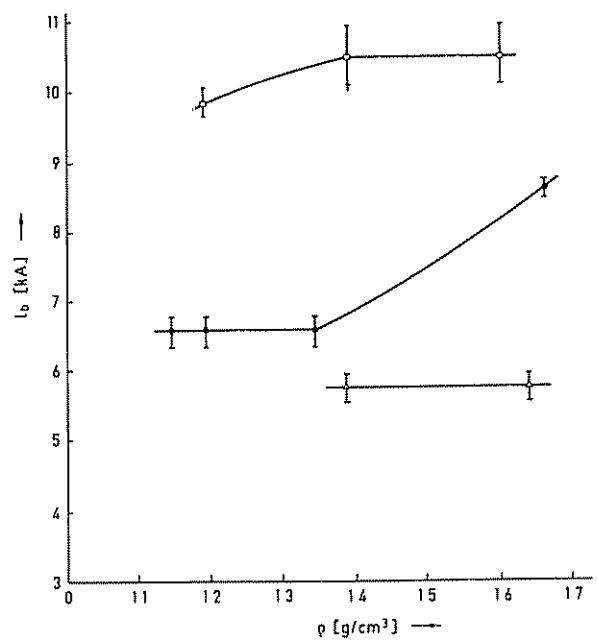

Figure 8. Burst current, I_b, at initiation threshold versus explosive density. ○ – Grain size 5 μm, Cu-foil 8.0 μm and flyer thickness 350 μm. • – Grain size 5 μm, Cu-foil 8.0 μm and flyer thickness 177.8 μm. △ Grain size 5 μm, Cu-foil 8.0 μm and flyer thickness 116.8 μm.

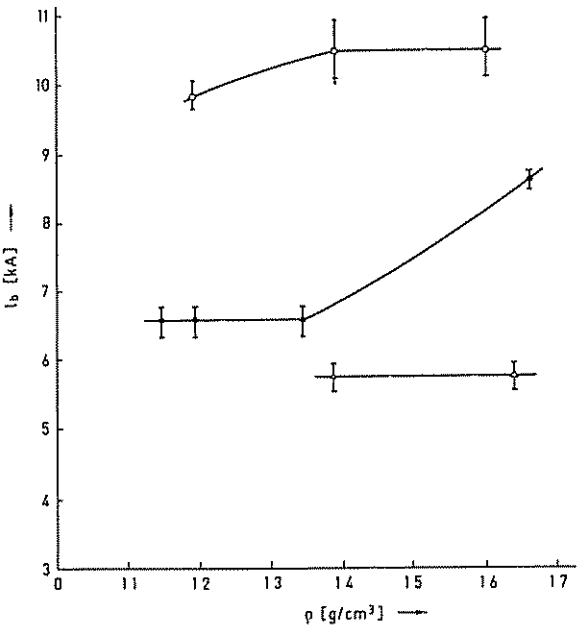

Figure 9. Burst power, P_b, at initiation threshold versus explosive density (see Fig. 8).

The flyer velocity can be controlled by adjusting the burst current density between 0.7 mm/μs to 2.5 mm/μs as in Fig. 3. Using the data we calculated the pressures generated by the flyer (kapton or Mylar) impact on the explosive pellet by impedance matching method, using the Hugoniot curves[7, 10] of each material. The shock initiation threshold of HNAB has been measured for pulses duration between 40 ns and 210 ns as determined by the flyer plates thickness, d, (76.2 μm to 350 μm). The impact duration τ is given by $\tau \simeq 2d/U_s$ where U_s is the shock velocity in the flyer plate. The initation threshold pressure versus impact duration for various bulk densities of the explosive is plotted in Fig. 10.

We examined the dependence of the critical energy for initiation upon the shock duration, τ, to see if the critical energy (or $P^2\tau$ = constant) can be taken as a shock initiation threshold criteria[11]. The results clearly indicate that as the duration of the initiating pulse gets longer, the threshold curve swings away from the curve $P^2\tau$ = constant (see Fig. 10). For long pulses the initiation criterion approaches one of a constant pressure, (as previously indicated by Schwarz in Ref. 1).

The constant threshold pressures (from the results of 350 μm flyer plates) were 2.9 GPa at a density of 1.6 g/cm^3, 2.2 GPa at 1.4 g/cm^3 and 1.9 GPa at 1.2 g/cm^3 (see Fig. 10).

We reach the conclusion that at short pulse duration the critical energy for initiation is smaller than that at long pulse duration. At density 1.6 g/cm^3 and thin flyer (76.2 μm corresponding to 42 ns pulse duration), the critical energy for initiation is 12 J/cm^2. This critical energy gets larger at longer pulse durations. For instance, with a flyer of 350 μm thickness (200 ns pulse duration), the critical energy is 36 J/cm^2.

The initiation threshold using a 76 μm flyer thickness requires less electrical energy in the storage capacitor compared to a thicker flyer, although the efficiency of energy transfer from electrical to kinetic energy of the flyer, is lower for thinner flyers (for constant foil thickness).

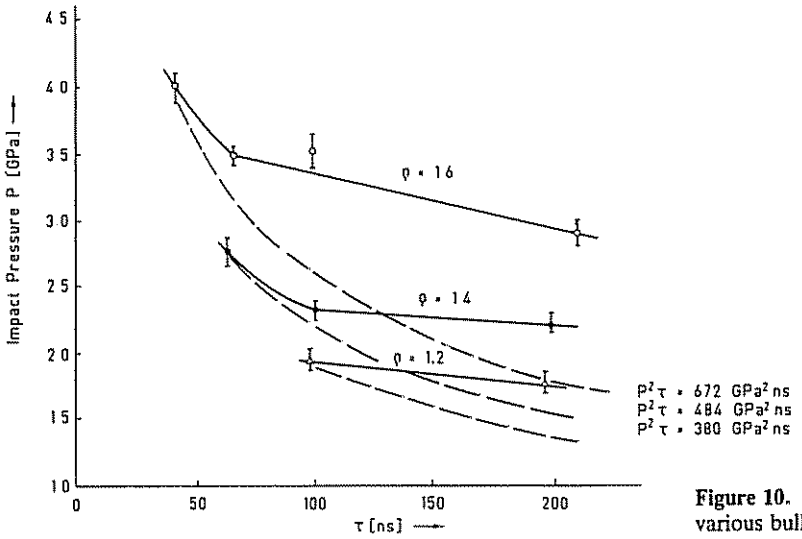

Figure 10. Threshold input pressure P, versus pulse duration, τ, for various bulk density of HNAB, (5 μm grain size, see Fig. 8).

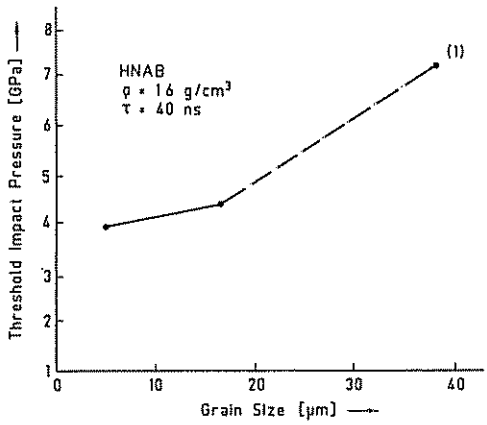

Figure 11. Threshold impact pressure, P, versus grain size

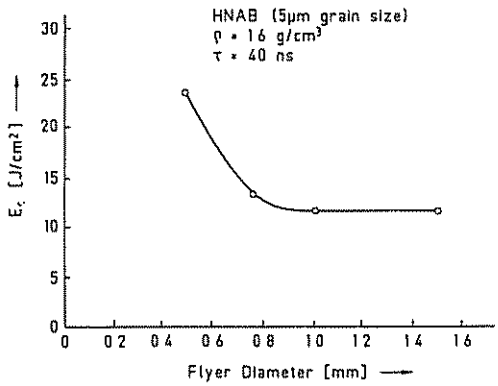

Figure 12. The critical energy, E_c, for initiation versus flyer diameter.

The powder morphology plays a significant role in the shock initiation sensitivity of HNAB. The initiation threshold versus grain size is given in Fig. 11. It indicates that the threshold increases with the explosive grain size, as can be expected from the hot spot model[12] that the number of reaction sites is larger for an explosive with fine grain size.

In Fig. 12 we plotted the critical initiation energy, E_c, as a function of flyer diameter. The plateau range indicates the existence of a minimum value, independent of the flyer diameter, for the critical energy which is required to initiate the explosive with constant flyer thickness, explosive density and grain size.

The initiation threshold rises dramatically as flyer diameter decreases below 0.75 mm; it can be explained by existing edge effects and initiation spot size effects. This phenomenon is probably related to the failure diameter of HNAB[13].

Our data, as shown in Figs. 8, 9 and 10, indicate that the initiation threshold pressure depends on the explosive density.

This relation can be explained by the fact that at low explosive density, the volume of the voids (reaction sites) is larger than at high explosive density, therefore the temperatures of reaction sites (hot spots model[12]), are increased due to adiabatic compression produced by the impacting flyer. The result is that the initiation threshold pressure at low density is lower than for a high density explosive (with the same grain size). This explanation is supported by experimental results obtained by Campbell et al.[14].

A second explanation based on a porous material concept as was shown by Zeldovich and Raizer[8]: For a given impact pressure, the difference between the two Hugoniot curves of porous and non-porous (continuous) explosives causes higher temperature in the porous explosives than in non-porous explosives.

5. Conclusion

The goal of this work was to study the shock initiation threshold of HNAB explosive. The main achievements are as follows:

(1) Development of electric gun for high impact pressure studies.
   a) Development of semi-empirical model of the exploding foil and comparison with the experimental data.
   b) The flyer plates were accelerated up to a velocity of 2.5 mm/μs generating impact pressures up to 7.3 GPa.

(2) The shock initiation threshold of HNAB has been measured.
   a) The curve of the energy threshold for initiation of HNAB swings away from $P^2\tau$ = const, as the pressure duration gets longer and becomes one of a constant pressure.
   b) Decreasing the density or grain size of the explosive reduces the impact pressure threshold.

c) The effect of the explosived density and grain size on initiation threshold can be explained by hot spots model and porous material concept.
d) The critical initiation energy as a function of flyer diameter was measured.

6. References

(1) A. C. Schwarz, *"Study of Factors which influence the Shock Initiation Sensitivity of HNS"*, Contract DE-AC04-76DP00789, Sandia Lab. Albuquerque, N.M. 87115, March 1981.
(2) A. C. Schwarz, *"Application of HNS in Explosive Components"*, Tech. Rep. SC-RR-71, Sandia Lab. Albuquerque, N.M. 87115, May 1972.
(3) E. Hasman, M. Gvishi, Z. Segelov, Y. Carmel, D. Ayalon, and A. Solomonovici, *"Acceleration of Flyer Plate by Electrically Exploded Foils and Application to Shock Initiation"*, Israel Physical Society, Jerusalem, April 1984.
(4) E. Hasman, M. Gvishi, Z. Segelov, Y. Carmel, D. Ayalon, and A. Solomonovici, "Shock Initiation of HNAB by Electrically Driven Flyer Plates", *The 8th Symposium (International) on Detonation*, Albuquerque, N.M., July 15, 1985.
(5) H. H. Chau, G. Dittbenner, W. W. Hofer, C. A. Honodel, D. J. Steinberg, R. J. Stroud, R. C. Steingart, and R. S. Lee, "Electric Gun: A Versatile Tool for High-pressure Shock-wave Research", *Rev. Sci. Inst. 51*, 1676 (1980).
(6) T. J. Tucker and P. L. Stanton, "Electrical Gurney Energy: New Concept of Modeling Energy Transfer from Electrically Exploded Conductors", Tech. Rep. SAND 75-0244, May 1975.
(7) E. Hasman, M. Sc. Thesis, Israel Institute of Technology, Technion, Haifa (1985).
(8) Ya, B. Zeldovich and Yu P. Raizer, *"Physics of Shock Waves and High Temperatures Hydrodynamic Phenomena"*, Academic Press, Inc., New York 1966.
(9) L. V. Altshuder, "Use of Shock Waves in High Pressure Physics", *Sov. Phys. Uspekhi* (Engl. Transl.) *8*, 52 (1965).
(10) L. M. Lee and A. L. Schwarz, "Shock Characterization of HNAB", *7th Symposium (International) on Detonation*, Annapolis Md., June 16, 1981.
(11) F. E. Walker and R. J. Wasley, "Critical Energy for Shock Initiation for Heterogeneous Explosives", *Explosivstoffe 17*, (1) 9 (1969).
(12) E. L. Lee and C. M. Tarver, "Phenomenological Model of Shock Initiation in Heterogeneous Explosives", *Phys. Fluids 23*, (12) December 1980.
(13) A. W. Campbell and R. Engelke, "The Diameter Effect in High Density Heterogeneous Explosives", *6th Symposium (International) on Detonation*, San Diego, CA., August 24, 1976.
(14) A. W. Campbell, Woc Davies, and J. R. Travis, "Shock Initiation of Detonation in Liquid Explosives", *Phys. Fluids 4*, 498 and 511 (1961).

Acknowledgements

We are grateful to Dr. Y. Me-Bar for his valuable and instructive comments. We wish to thank Mr. I. Mispe and his group and Mr Z. Sundak for their technical assistance. Our thanks are also due to Mrs. D. Ayalon and Dr. A. Solomonovici for the preparation of HNAB pellets.

(Received February 6, 1986; Ms 5/86)